Tree Density Estimation Using a Distance Method in Mali Savanna

Nicolas Picard, Amadou M. Kouyaté, and Hélène Dessard

ABSTRACT. The biological characteristics of trees in tropical dry savannas make it difficult to conduct inventories of tree density, and this has aroused interest in distance-based methods. This study proposes a distance-based tree density estimator using Matérn point processes, generating clustered spatial patterns. It was defined as the maximum likelihood estimator of the density, based on an approximate distribution of the distance from a random point to the pth nearest tree. It was compared with seven estimators identified in the literature as the most efficient. The estimators were compared on a benchmark of 10 point processes, with six being adjusted to observed tree patterns in six Mali savannas (West Africa). The proposed estimator was generally the most efficient. However, this result ignores that (i) all estimators do not require the same effort on the field, (ii) the point-processes benchmark was restricted to Matérn processes, and (iii) all estimators are not equivalent with respect to measurement errors. FOR. SCI. ():.

Key Words: Distance sampling, density-adapted sampling, tropical dry forest, Matérn process, spatial pattern.

WOOD AND CHARCOAL IN MALI (WEST AFRICA) account for more than 90% of domestic energy (Nouvellet et al. 2000), and the tree formations (mainly savannas) are thus subject to a high level of exploitation. Since 1998, the government in Mali has encouraged the creation of so-called "rural markets for fuel wood," and these rely on the definition of a management plan for village forests, that in turn requires an assessment of the wood stock. Classical inventory techniques are difficult to use in dry savannas because of the shrub aspect of the trees (small trees, many stems on each stump, curved shape of the stems with many ramifications, etc.) Moreover, budgets available for forest inventory are small, and the operators in charge of the inventories are rarely well trained.

All these considerations have led in Mali to distance-based forest inventory methods (Kouyaté 1995, Sylla 1997), that are supposed to be easy and fast to apply (Lindsey et al. 1958, Lessard et al. 2002, Lynch and Rusydi 1999). Figure 1 gives the distances D, the most frequently measured in distance-based methods. Let p be the fixed number of trees in each sampling plot, and $S(D)$ its variable area. We denote as λ the tree density. An estimator of the tree density is: $\hat{\lambda} = p/S(D)$. The difficulty is that the expected value of $1/S(D)$, and thus that of $\hat{\lambda}$, depends on the spatial pattern of the trees. A spatial pattern will be considered as the realization of a point process (Cressie 1991, Stoyan and Stoyan 1994). Let $f(\cdot, \theta)$ be the density function of the distance D for a point process with parameters θ (among which is the intensity λ). To estimate θ, authors generally use the maximum likelihood estimator, or the m-order moment estimator that follows from

$$\frac{1}{n}\sum_{i=1}^{n} D_i^m = \int_0^\infty x^m f(x, \hat{\theta})\, dx$$

where $D_1, \ldots, D_n$ is a sample of size n of D. For homogeneous Poisson process with intensity λ, the expected value

Nicolas Picard, Cirad-forêt, BP 1813, Bamako, Mali—Phone: (+223) 224 64 28; Fax: (+223) 221 87 17; nicolas.picard@cirad.fr. Amadou M. Kouyaté, Institut d'Économie Rurale, BP 258, Bamako, Mali—Phone: (+223) 224 64 28; amadou.kouyate@ier.ml. Hélène Dessard, Cirad-forêt, Campus International de Baillarguet, TA 10/D, 34398 Montpellier Cedex 5, France—Phone: (+33) 467 615 800 ext.4209; helene.dessard@cirad.fr.

Acknowledgments: We would thank the Associate Editor and three anonymous reviewers for helpful comments on the manuscript.

Manuscript received March 31, 2003, accepted August 19, 2004.

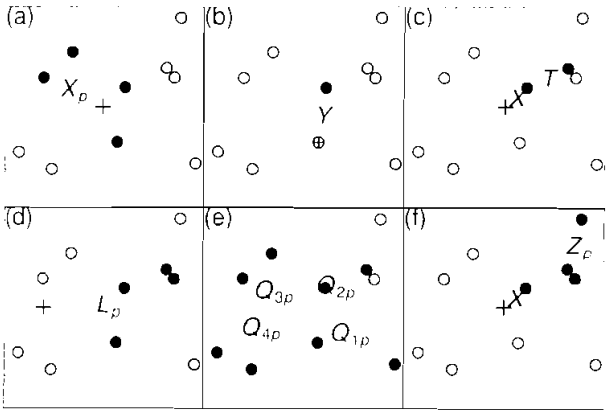

Figure 1. Distances most commonly measured in distance-based methods: (a) X_p is the distance from the sampling point to the pth nearest tree (here $p = 4$). (b) Y is the distance from a randomly chosen tree to its nearest neighbor. (c) Let A be the nearest tree from the sampling point E; T is the distance from A to its nearest neighbor in the half-plane that excludes E and limited by the perpendicular to (AE) at A. (d) L_p is the distance from sampling point E to the pth nearest tree in a transect of fixed width that starts at E (here $p = 4$). (e) Q_{kp} is the distance from the sampling point to the pth nearest tree located in the kth sector, the plane being divided into m equal sectors (here $m = 4$ and $p = 2$). (f) Z_p is the distance from tree A_p to its nearest neighbor A_{p+1}, the trees $A_1, \ldots, A_{p-1}$ being excluded, and A_1 being the nearest tree from the sampling point (here $p = 3$).

of X_p^m, where X_p is the distance from the sampling point to the pth nearest tree (Figure 1a), is proportional to $\lambda^{-m/2}$ (Stoyan and Stoyan 1994). So, referring to Persson's (1971) classification, the first-order moment estimator of the density for a Poisson process belongs to the type $(1/\Sigma X)^2$, the second-order moment estimator is of type $1/(\Sigma X^2)$, and the moment estimator of order -2 is of type $\Sigma(1/X^2)$. Moreover, for a homogeneous Poisson process, the maximum likelihood estimator based on X_p is identical, up to a multiplicative factor, to the second-order moment estimator. Table 1 gives the most commonly found estimators, crossing the type of distance measured (Figure 1) and Persson's (1971) classification.

Most of these estimators were designed for the Poisson process, though some were designed for point processes that generate regular grids (square, triangular, hexagonal, etc.), whereas others were designed to be robust. However, to the best of our knowledge, no estimator has been devoted to a point process that generates clustered patterns. However, trees in natural forest stands, and, in particular, in the tree savannas of Mali, generally have a clustered spatial pattern. This study therefore aimed to define a tree density estimator for clustered patterns; and test this estimator at six sites in Mali. To reach this goal, the ideal situation would be to use a clustering point process that can be simulated and for which the distribution of the distance D is known. Unfortunately, we are not aware of such a process. Clustering point processes that can be simulated have untractable characteristics. In contrast, the known distributions of D for clustered patterns correspond to point patterns whose generating processes are unknown (Eberhardt 1967). Some approximations therefore had to be made. We relied on the family of Matérn point processes to generate clustered patterns, and then approximated the distribution of D by known distributions. A tree density estimator could then be deduced and was compared with other estimators given in the literature.

Material and Methods

Matérn Process

Matérn processes are three-parameter point processes that generate clustered spatial patterns. The three parameters consist of dispersion distance R, density of parent points ω, and mean number of daughter point per parent μ. The process is then defined as follows (Stoyan and Stoyan 1994): 1. Parent points are drawn according to a homogeneous Poisson process with density ω; 2. Each parent point i generates M_i daughter points, where the M_is are independent and identically distributed according to a Poisson distribution with parameter μ; 3. The M_i daughters of each parent point are uniformly distributed in the disk of radius R centered on the parent point. The Matérn field is finally formed by the union of all daughter points.

The density of a Matérn process with parameters (R, ω, μ) is $\lambda = \omega\mu$. The key point in distance method density estimation is the distribution function F_p of the distance X_p from a random point to the pth nearest neighbor. The analytic expression of F_p for $p = 1$ is (Stoyan and Stoyan 1994)

$$F_1(x) = 1 - exp\left\{ -2\pi\omega \int_0^{R+x} t\left[1 - \exp\left(-\frac{\mu a(t, x, R)}{\pi R^2}\right)\right] dt \right\},$$

where $a(t, x, R)$ is the area of intersection of two disks of radius x and R separated by a distance t. The expression of a is (Stoyan and Stoyan 1994)

$$a(t,r,R) = \begin{cases} \pi \min(r, R)^2 & \text{for } t \le |r - R| \\ r^2(\arccos u - u\sqrt{1 - u^2}) & \text{for } |r - R| < t < R + r \\ \quad + R^2(\arccos v - v\sqrt{1 - v^2}) & \\ 0 & \text{for } t \ge R + r \end{cases} \quad (1)$$

$$u = \frac{t^2 - r^2 - R^2}{2tr} \qquad v = \frac{t^2 + R^2 - r^2}{2tR}.$$

Because we do not have any explicit expression of F_p for $p \ge 2$, an approximate expression is derived. As noticed by Eberhardt (1967), F_p is defined by the law of the number of trees in plots, because

$$F_p(x) = Pr(X_p \le x) = \sum_{i=p}^{\infty} p_i(x) = 1 - \sum_{i=0}^{p-1} p_i(x), \quad (2)$$

Table 1. The distance-based density estimators most commonly found in the literature.

Citation	Type of Distance	Type of Estimator	Citation	Type of Distance	Type of Estimator
Moore (1954)[a]	X_1	$1/(\Sigma X^2)$	Holgate (1965b)[a]	Y	$1/(\Sigma X^2)$
Morisita (1954)[a]	—	—	Diggle (1975, 1977)[k]	—	—
Batcheler (1971)[l]	—	—	Cottam and Curtis (1956)[i]	—	$(1/\Sigma X)^2$
Diggle (1975, 1977)[k]	—	—	Pollard (1971)[a]	$Q_{1/2}$	$1/(\Sigma X^2)$
Cottam and Curtis (1956)[i]	—	$(1/\Sigma X)^2$	Morisita (1954)[i]	—	$(1/\Sigma X)^2$ [b]
Persson (1964)[i]	—	—	Cottam and Curtis (1956)[i]	—	—
Holgate (1965a)[i]	—	—	Catana (1963)	—	—
Persson (1971)[i]	—	—	Mawson (1968)[a]	$Q_{1/2}$	$1/(\Sigma X^2)$
Patil et al. (1979, 1982)[g]	—	other	Engeman et al. (1994)[c]	—	—
Clayton and Cox (1986)[d]	—	—	Morisita (1957)[a]	—	$\Sigma(1/X^2)$
Morisita (1954)[m]	$X_{1/2}$	$1/(\Sigma X^2)$	Engeman et al. (1994)[c]	—	—
Thompson (1956)[m]	—	—	Mawson (1968)[n]	—	other
Keuls et al. (1963)[a]	—	—	Kendall and Moran (1963)[a]	Z_1	$1/(\Sigma X^2)$
Holgate (1964)[a]	—	—	Cox (1976)[l]	—	
Pollard (1971)[a]	—	—	Clayton and Cox (1986)[f]	—	—
Sylla (1997)[c]	—	—	Cox (1976)[l]	—	$\Sigma(1/X^2)$
Keuls et al. (1963)[b,i]	—	$\Sigma(1/X^2)$	Cottam and Curtis (1956)[c]	—	$(1/\Sigma X)^2$
Persson (1964)	—	—	Clayton and Cox (1986)[f]	—	—
Eberhardt (1967)[b]	—	—	Clayton and Cox (1986)[d]	—	other
Mawson (1968)[b]	—	—	Engeman et al. (1994)[a]	$Z_{1/2}$	$1/(\Sigma X^2)$
Prodan (1968)[c]	—	—	Diggle (1975, 1977)[k]	T	$1/(\Sigma X^2)$
Payandeh and Ek (1986)	—		Aherne and Diggle (1978)[k]	—	—
Jonsson et al. (1992)	—	—	Clayton and Cox (1986)[f]	—	—
Lynch and Rusydi (1999)	—	—	Byth (1982)[l]	—	$(1/\Sigma X)^2$
Lessard et al. (2002)[b]	—	—	Clayton and Cox (1986)[f]	—	—
Morisita (1954)[f]	—	$(1/\Sigma X)^2$	Engeman et al. (1994)[f]	—	—
Thompson (1956)[f]	—	—	Clayton and Cox (1986)[d]	—	other
Lewis (1975)	—	—	Parker (1979)[a]	L	$1/(\Sigma X^2)$
Payandeh and Ek (1986)	—	—	Parker (1979)[h]	—	$\Sigma(1/X^2)$
Persson (1964)[c]	—	other	Sheil et al. (2003)[f]	—	—
Lewis (1975)[d]	—	—	Smaltschinski (1981)[h]	$X_{1/2}$	other

The definition of distance types refers to Figure 1. The estimators classification refers to Persson (1971).

[a] Estimator not biased for a homogeneous Poisson process.

[b] Estimator not biased for Poisson processes (homogeneous or not) and when the number of trees in a plot of any size follows a binomial or a negative binomial distribution.

[c] Estimator based on the median of $X_{1/2}$. An asymptotically nonbiased expression of this exists for the homogeneous Poisson process and for the processes that generate regular grids.

[d] Robust estimator, of the type $1/(\Sigma X^c)^{2/c}$, where c is a fixed coefficient, $c = -1$ is the type $(1/\Sigma X)^2$, $c = 2$ is the type $1/(\Sigma X^2)$, and $c = -2$ is the type $\Sigma(1/X^2)$.

[e] Empirical estimator.

[f] Robust estimator.

[g] Robust estimator of $f(0)$, based on a rank statistic, where f is the density function of πX^2.

[h] Estimator defined as a combination of the arithmetic and harmonic means of $X_{1/2}$.

[i] Estimator of $1/\lambda$ not biased for homogeneous Poisson processes.

[j] Estimator of $1/\lambda$ not biased for the processes that generate regular grids (square, triangular, hexagonal, etc.).

[k] Estimator of $1/\lambda$ not biased for homogeneous Poisson processes.

[l] Estimator based on truncated distances.

[m] Maximum likelihood estimator of a homogeneous Poisson process.

[n] Estimator of the type $\Sigma[1/(\Sigma_i Q_{i/2})]$.

where $p_i(x)$ is the probability of finding i trees in the disk of radius x centered on the origin (or any other point). Then, any approximate expression of $p_i(x)$ for a Matérn process also defines an approximate expression of F_p.

An approximate expression of $p_i(x)$ was derived from simulation data and empirical relationships. We simulated 512 Matérn processes for R values ranging from 1 to 8 m, for ω values ranging from 100 to 800 ha^{-1} and for μ values ranging from 1 to 8. Each process was simulated 10,000 times on a 1-ha plot, and for each iteration we counted the number of trees in 100 disks ranging from $\pi x^2 = 1$ m^2 to 1 ha in size. For each combination of (R, ω, μ) and for each value of x, we thus obtained a sample of 10,000 values for the number of trees in the disk of radius x. An estimate of $p_i(x)$ was thus obtained for each of the 512 Matérn processes. We then empirically noticed, like Eberhardt (1967), that $p_i(x)$ was closely approximated by a negative binomial distribution with parameters (m, k)

$$p_i(x) = \frac{\Gamma(k+i)}{\Gamma(k)\Gamma(i+1)} \frac{m^i k^k}{(m+k)^{k+i}}, \qquad (3)$$

where Γ is the gamma function (Abramowitz and Stegun 1964). The parameter m is the mean number of trees in the disk of radius x, so that: $m = \lambda\pi x^2 = \omega\mu\pi x^2$. The relationship between the shape parameter k and the process parameters (R, ω, μ) were empirically derived from the

simulation data by visual analysis and by testing various relationships. The resulting relationship is

$$k = (a_0 + a_1 R)\omega + (a_2/\mu)\, m, \qquad (4)$$

where a_0, a_1, and a_2 are constant coefficients. Equations 2–4 thus define an approximate expression of F_p for a Matérn process. It should also be noted that we do not know the generating process of the point process whose distribution of X_p would be given exactly by Equations 2–4.

The coefficients a_0, a_1, and a_2 were estimated from the simulation data by minimizing, for a given order p, the quantity

$$\sum_{q=1}^{512} \int_0^{\infty} [F_{pq}^{\text{sim}}(x) - F_{pq}(x; a_0, a_1, a_2)]^2\, dx,$$

where the sum is over the 512 simulated Matérn processes, F_{pq} is the distribution function of X_p for the qth Matérn process computed from the coefficients a_0, a_1, a_2 using Equations 2–4, and F_{pq}^{sim} is the empirical distribution function estimated from the sample of size 10,000 of X_p for the qth Matérn process.

Definition of the Density Estimator

The density estimator we propose is the maximum likelihood based on a sample of the distance X_p from a random point to the pth nearest tree. The expression of the likelihood is actually approximate, because it is based on the approximate expression of the distribution function F_p of X_p for the Matérn processes. It follows from Equation 2 that the expression of the log-likelihood for a sample $x_1, \ldots, x_n$ of size n of X_p is

$$\mathcal{L}(x_1, \ldots, x_n) = \sum_{i=1}^{n} \ln\left[-\sum_{i=0}^{p-1} p_i'(x_i) \right]. \qquad (5)$$

Then follows from Equations 3 and 4 the expression of the derivative p_i' of p_i with respect to x. It is actually more convenient to compute the derivative of $\ln[p_i(x)]$, which yields

$$p_i'(x) = p_i(x) m' \left\{ \frac{a_2}{\mu} \left[\psi(k+i) - \psi(k) - \ln\left(1 + \frac{m}{k}\right) \right] + \frac{(a_0 + a_1 R)\omega}{m+k} \left(\frac{i}{m} - 1 \right) \right\}, \qquad (6)$$

where Ψ is the digamma function (Abramowitz and Stegun 1964) and $m' = 2\omega\mu\pi x$ is the derivative of m with respect to x. Equation 6 is valid for $x > 0$; moreover $p_i'(0) = 0$. Let $(\hat{R}, \hat{\omega}, \hat{\mu})$ be the value of (R, ω, μ) that maximizes $\mathcal{L}(x_1, \ldots, x_n)$. Then the proposed tree density estimator is $\hat{\lambda} = \hat{\omega}\hat{\mu}$.

In practice, Equation 5 is maximized numerically. We used the Nelder–Mead algorithm (Nelder and Mead 1965) in R software (R Development Core Team 2003). This algorithm, like most optimization algorithms, requires some initial values of R, ω, and μ. When estimating density from a simulated data set of a known Matérn process, it is of course possible to use the true values of R, ω, and μ as the initial values. However, the initial values may have an effect on the numerical output, and a better simulation of field conditions is obtained if we proceed as if the true values were unknown. First, we used as an initial density value $\omega\mu$, that value given by the moment estimator of order -2 of a Poisson process (see Equation 13). Let $\hat{\lambda}_{-2}$ be this estimate. Then, we used the simulation data to derive some empirical expressions for the initial values of R, ω, and μ. For each of the 512 simulated Matérn processes, we computed the empirical mean $\hat{m}$ and the empirical standard deviation $\hat{\sigma}$ of X_p from its sample of size 10,000. We then constructed the linear regressions

$$\hat{m}_q = \beta_0 + \beta_\omega \omega_q + \beta_\mu \mu_q + \varepsilon_q, \qquad (7)$$

$$\hat{\sigma}_q = \alpha_0 + \alpha_\omega \omega_q + \alpha_\mu \mu_q + \alpha_R R_q + \varepsilon_q, \qquad (8)$$

where $q = 1, \ldots, 512$ refers to the simulated Matérn processes. Once the coefficients of these regressions are known, the initial values of R, ω, and μ are obtained for any point process by solving $\hat{m} = \beta_0 + \beta_\omega \omega + \beta_\mu \mu$, $\hat{\sigma} = \alpha_0 + \alpha_\omega \omega + \alpha_\mu \mu + \alpha_R R$, and $\hat{\lambda}_{-2} = \omega\mu$, where $\hat{m} = (\sum_{i=1}^{n} x_i)/n$ and $\hat{\sigma}^2 = [\sum_{i=1}^{n}(x_i - \hat{m})^2]/(n-1)$ are the estimated mean and variance of a sample $x_1, \ldots, x_n$ of X_p. This yields

$$\mu_{\text{init}} = [\hat{m} - \beta_0 - \sqrt{(\hat{m} - \beta_0)^2 - 4\beta_\mu \beta_\omega \hat{\lambda}_{-2}}]/(2\beta_\mu), \qquad (9)$$

$$\omega_{\text{init}} = \hat{\lambda}_{-2}/\mu_{\text{init}}, \qquad (10)$$

$$R_{\text{init}} = (\hat{\sigma} - \alpha_0 - \alpha_\omega \omega_{\text{init}} - \alpha_\mu \mu_{\text{init}})/\alpha_R. \qquad (11)$$

Because regressions 7 and 8 were constructed for a limited range of R, ω, and μ, the initial values of R, ω, and μ were actually $\min[\max(R_{\text{init}}, 1), 8]$ (in m), $\min[\max(\omega_{\text{init}}, 0.01), 0.08]$ (in m^{-2}), and $\min[\max(\mu_{\text{init}}, 1), 8]$.

Study Sites

The distance method for estimating tree density was assessed at six sites in Mali, West Africa (Table 2). One of the sites (Amba) is located in the South Sahelian bioclimatic range (Nasi and Sabatier 1988), another (Woro) is located in the North Sudanese range, and the four remaining sites are located in the South Sudanese range. The vegetation at all the sites consists of tree savanna (Yangambi classification, Conseil Scientifique pour l'Afrique 1956). A 50 × 100-m permanent plot was located at random at each site. The species, girth, and spatial coordinates of all the trees and shrubs with a base girth >10 cm were recorded. Spatial coordinates were measured with a tape after dividing the plot into 10 × 10-m subplots bounded by string. Plot characteristics are given in Table 2: density ranged from 198 to 1486 ha^{-1} and basal area ranged from 2.8 to 12.5 m^2ha^{-1}. Rainfall explains the differences between the plots, whereas, more locally, human activities had a marked impact on plot characteristics.

A Matérn process was adjusted to each observed spatial pattern. Its density was estimated as $\lambda = N/W$ where N is the

Table 2. Characteristics of the six study sites in Mali, West Africa

Site	Longitude W	Latitude N	Pluviometry[a] mm yr^{-1}	Density ha^{-1}	Basal area m^{2}ha^{-2}	Species Richness
Amba	3°30′	15°15′	280	198	2.8	7
Kokani	8°28′	12°24′	800	600	10.9	30
Korokoro	7°24′	12°45′	790	1,348	8.4	29
Ndouantien	7°17′	12°46′	790	1,486	7.3	38
Sokouna	7°18′	12°52′	790	790	12.5	32
Woro	7°29′	13°41′	570	364	5.2	15

[a] Average from 1977 to 1987; data from the nearest meterological station.

number of trees in the plot and $W = 0.5$ ha. The other parameters were estimated using the minimum-contrast method (Stoyan and Stoyan 1994), which is efficient and takes advantage of knowledge concerning tree position. This consists of minimizing, with respect to R and ω, the quantity

$$\int_0^{r_{\max}} [\hat{K}(r)^\gamma - K(r, R, \omega)^\gamma]^2 \, dr,$$

where $r_{\max} = 25$ m, $\gamma = 0.25$, $\hat{K}$ is Ripley's estimator of his K function (Cressie 1991), and $K(r, R, \omega)$ is Ripley's K function for a Matérn process with parameters (R, ω, μ). Its expression is (Stoyan and Stoyan 1994)

$$K(r, R, \omega) = \pi r^2 + \frac{1}{\omega}$$

$$\begin{cases} 2 + (1/\pi)[(8z^2 - 4)\arccos z - 2\arcsin z \\ \quad + 4z\sqrt{(1 - z^2)^3} - 6z\sqrt{1 - z^2}] & (z \le 1) \\ 1 & (z > 1), \end{cases}$$

where $z = r/(2R)$. It should be noted that K does not depend on μ. This latter parameter is estimated as $\hat{\mu} = \lambda/\omega$.

Comparison with Other Estimators

Several authors have compared the performance of distance-based estimators with fixed-sized sample plot estimators (Moore 1954, Lindsey et al. 1958, Holgate 1964, Eberhardt 1967, Pollard 1971, Engeman et al. 1994, Lessard et al. 1994, Lynch and Rusydi 1999, Lessard et al. 2002). In all cases, distance-based estimators had a higher standardized root squared error than sample plot estimators. Other authors have made pairwise comparisons of the performance of distance-based estimators (Diggle 1975, 1977, Cox 1976, Clayton and Cox 1986, Payandeh and Ek 1986, Jonsson et al. 1992, Engeman et al. 1994, Engeman and Sugihara 1998). Estimators of the type $\Sigma(1/X^2)$ (Table 1) were generally more robust than estimators of the type $1/(\Sigma X^2)$ (Persson 1964, Eberhardt 1967, Payandeh and Ek 1986, Jonsson et al. 1992), but the lower value of their bias was compensated by the higher value of their variance.

The performance of the proposed estimator $\hat{\omega}\hat{\mu}$ was assessed in comparison with distance-based estimators recognized in the literature as the most efficient. We in fact followed the conclusions of three studies that encompassed all the other comparative studies. Following Clayton and Cox's (1986) conclusions, we selected the three estimators $\hat{\lambda}_5$, $\hat{\lambda}_6$, and $\hat{\lambda}_7$ proposed by these authors

$$\hat{\lambda}_5 = \frac{n^2(0.35 + 0.01m_2/n)}{(\sum_{i=1}^{n} X_i)(\sum_{i=1}^{n} Z_i)},$$

$$\hat{\lambda}_6 = \frac{n^2(0.44 - 0.08m_2/n)}{(\sum_{i=1}^{n} X_i)(\sum_{i=1}^{n} T_i)}, \qquad (12)$$

$$\hat{\lambda}_7 = \frac{n^2(0.45 - 0.08m_{1.5}/n)}{(\sum_{i=1}^{n} X_i)(\sum_{i=1}^{n} T_i)},$$

where X_i is the distance from the ith (within a sample of size n) sampling point, say E, to the nearest tree, say A (Figure 1a), T_i is the distance from A to its nearest neighbor in the half-plane that excludes E and limited by the perpendicular to (AE) at A (Figure 1e), Z_i is the distance from A to its nearest neighbor (Figure 1f), and m_r is the number of pairs (X_i, Z_i) or (X_i, T_i) out of the n measured pairs for which $Z_i > rX_i$ or $T_i > rX_i$. Following Payandeh and Ek's (1986) conclusions, we also selected the moment estimator of order -2 of a Poisson process (Keuls et al. 1963, Persson 1964, Eberhardt 1967, Mawson 1968, Jonsson et al. 1992, Lessard et al. 2002)

$$\hat{\lambda}_{-2} = \frac{p - 1}{\pi n} \sum_{i=1}^{n} \frac{1}{X_{pi}^2}, \qquad (13)$$

where X_{pi} is the distance from the ith sampling point to the pth nearest tree (Figure 1a). Finally, following Engeman et al.'s (1994) conclusions, we selected three more estimators: Kendall–Moran's estimator, the second-order moment estimator for a Poisson process, and the variable area transect estimator. The Kendall–Moran estimator is defined as follows (Kendall and Moran 1963, Engeman et al. 1994): let A_1 be the nearest tree from the sampling point E, and let A_{p+1} $(p \ge 1)$ be the nearest tree from A_p disregarding $A_1, \ldots, A_{p-1}$ (Figure 1f); let Z_p be the distance from A_p to A_{p+1}, and finally let $\mathcal{A}_p$ be the area to explore to find A_p. This area is the area of union of the p disks centered at $E, A_1, \ldots, A_{p-1}$ with radii $X, Z_1, \ldots, Z_{p-1}$. Then the Kendall–Moran estimator of order p is

$$\hat{\lambda}_{KM} = \frac{np - 1}{\sum_{i=1}^{n} \mathcal{A}_{pi}}. \qquad (14)$$

The Kendall–Moran estimator is not, strictly speaking, a distance-based estimator because it cannot be computed from mere distance measurements. The second-order moment estimator for a Poisson process is (Morisita 1954, Thompson 1956, Keuls et al. 1963, Holgate 1964)

$$\hat{\lambda}_2 = \frac{np - 1}{\pi \sum_{i=1}^{n} X_{pi}^2}, \quad (15)$$

where X_{pi} was defined previously (see definition of $\hat{\lambda}_{-2}$). The variable area transect estimator is (Parker 1979, Sheil et al. 2003)

$$\hat{\lambda}_I = \frac{np - 1}{W \sum_{i=1}^{n} L_{pi}}, \quad (16)$$

where L_{pi} is the distance from the ith sampling point, say E, to the pth nearest tree in a transect of width W that starts at E (Figure 1d). In this study, we used $W = 10$ m.

We thus selected seven estimators for comparison with $\hat{\omega}\hat{\mu}$. The four estimators $\hat{\lambda}_{-2}$, $\hat{\lambda}_{KM}$, $\hat{\lambda}_2$, and $\hat{\lambda}_I$ are unbiased for a homogeneous Poisson process. The variance of the latter three then equals $\lambda^2/(np - 2)$, whereas the variance of $\hat{\lambda}_{-2}$ then equals $\lambda^2/[n(p - 2)]$. As a comparison, the variance of the fixed size sample plot estimator equals $\lambda^2/(np)$ for a plot size such that the plot contains p trees on average.

The seven estimators (Equations 12–16) and the proposed estimator $\hat{\omega}\hat{\mu}$ were compared on the basis of their standardized root squared error (Diggle 1977),

$$\rho(\hat{\lambda}) = \sqrt{E\{[(\hat{\lambda} - \lambda)/\lambda]^2\}}$$

$$= \sqrt{[\sigma(\hat{\lambda})/\lambda]^2 + [B(\hat{\lambda})]^2},$$

where $\sigma(\hat{\lambda})$ is the estimator standard deviation, and $B(\hat{\lambda})$ is its standardized bias (Diggle 1975),

$$B(\hat{\lambda}) = E[(\hat{\lambda} - \lambda)/\lambda] = E(\hat{\lambda})/\lambda - 1.$$

The smaller $\rho(\hat{\lambda})$, the more efficient $\hat{\lambda}$. The estimators were also compared on the basis of the mean exploration area required at each sampling point. For estimators $\hat{\omega}\hat{\mu}$, $\hat{\lambda}_2$, and $\hat{\lambda}_{-2}$, this was the mean value of πX_{pi}^2; for $\hat{\lambda}_{KM}$, it was the mean value of πI_{pi}; for $\hat{\lambda}_I$, it was the mean value of WL_{pi}; for $\hat{\lambda}_5$, it was the mean value of $\pi(X^2 + Z^2) - a(X, X, Z)$, where a is given by Equation 1; and, for $\hat{\lambda}_6$ and $\hat{\lambda}_7$, it was the mean value of $\pi(X^2 + T^2/2)$ (Figure 1).

The estimators were compared on a benchmark of ten reference point processes: the six Matérn processes corresponding to the six study sites, the Matérn process with parameters $R = 2$ m, $\omega = 100$ ha^{-1}, $\mu = 5$, the Matérn process with parameters $R = 5$ m, $\omega = 100$ ha^{-1}, $\mu = 5$, the Matérn process with parameters $R = 1$ m, $\omega = 500$ ha^{-1}, $\mu = 1$, and the Poisson process with intensity $\lambda = 500$ ha^{-1}. Point process simulations were used rather than plot data because the latter offered limited sampling possibilities, and therefore limited data sets. Each reference point process was simulated 10,000 times, and for each iteration the distances required for the estimators were computed. These data were partitioned into 200 samples of size 50. Thus 200 estimates $\lambda_1, \ldots, \lambda_{200}$ of the density based on a sample of size $n = 50$ were obtained for each estimator and each point process. The standardized bias was then computed as $B = \bar{\lambda}/\lambda - 1$, where $\bar{\lambda} = (\sum_{i=1}^{200} \lambda_i)/200$, and the standardized standard deviation was computed as $\sigma/\lambda = \sqrt{\lambda^2 - \bar{\lambda}^2}/\lambda$, where $\lambda^2 = (\sum_{i=1}^{200} \lambda_i^2)/200$.

Results

As suggested by Kouyaté (1995) and Sylla (1997), we focus hereafter on the order $p = 4$. The estimators $\hat{\omega}\hat{\mu}$, $\hat{\lambda}_2$, $\hat{\lambda}_{-2}$, and $\hat{\lambda}_I$ were thus assessed for $p = 4$. The Kendall–Moran estimator was assessed for $p = 3$ because it appears to be of little practical use in the field for $p > 3$. We first present some characteristics of the proposed estimator (parameter values, use with field data, effect of sample size), and then make comparisons with the other estimators.

Parameter Values

At the order $p = 4$, the numerical values of the coefficients a_0, a_1, a_2 corresponded to $a_0 = -16.4555$ m^2, $a_1 = 20.9673$ m, and $a_2 = 0.9242$. The results of regressions 7 and 8 from which the initial values of (R, ω, μ) were computed, are given for $p = 4$ in Table 3. Finally, Table 4 gives the values of the parameters (R, ω, μ) of the Matérn processes that best fit the observed spatial patterns at the six study sites.

Example of an Estimation from Field Data

We first provide an example of a density estimation using the proposed estimator and field data. These data were generated from stem maps: all the trees recorded on a plot were placed on x–y coordinates; sampling points were located on a regular square grid with sides a within the

Table 3. Linear regression of the empirical mean m_4 and the empirical standard deviation σ_4 of X_4 with respect to the parameters R, ω, and μ of the Matérn point process, for 512 processes.

Coefficient	Unit	Estimate	SE	T	$\Pr(>\|T\|)$
β_0	m	8.0505	1.159×10^{-1}	69.48	$<10^{-15}$
β_ω	m^{-1}	−54.1929	1.713×10^{-4}	−31.64	$<10^{-15}$
β_μ	m	-4.6170×10^{-1}	1.713×10^{-2}	−26.96	$<10^{-15}$
α_0	m	3.1407	4.776×10^{-2}	65.76	$<10^{-15}$
α_R	—	-7.2432×10^{-2}	5.879×10^{-3}	−12.32	$<10^{-15}$
α_ω	m^3	−23.1092	5.879×10^{-5}	−39.31	$<10^{-15}$
α_μ	m	-1.0824×10^{-1}	5.879×10^{-3}	−18.41	$<10^{-15}$

For regression 7, $R^2 = 77\%$; for regression 8, $R^2 = 80\%$.

Table 4. Values for parameters (R, ω, μ) of the Matérn processes that best fit the observed spatial patterns at the six study sites

Site	R m	ω ha^{-1}	μ
Kokani	2.07	494	1.215
Sokouna	10.2	70	11.343
Korokoro	1.77	1,036	1.177
Ndouantien	2.36	630	2.364
Woro	1.93	229	1.586
Amba	1.13	168	1.176

R is the dispersion distance, ω is the density of parent points, and μ is the mean number of daughter points per parent.

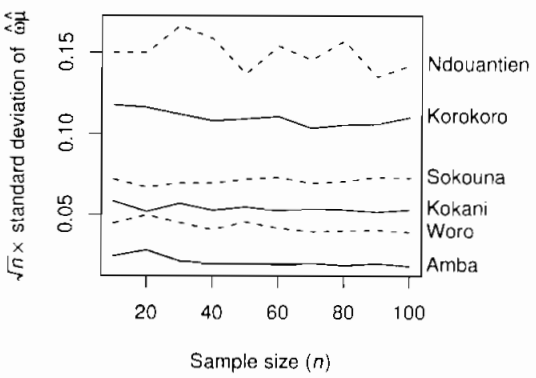

Figure 2. Empirical standard deviation σ of the proposed estimator $\hat{\omega}\hat{\mu}$ times $\sqrt{n}$ as a function of sample size n, at the six study sites.

coordinate system; the distance from each sampling point to the fourth nearest tree was also recorded. When dealing with field data, it must be ensured that sampling points are sufficiently spaced one from the other so that measured distances can be considered as independent, because a maximum likelihood estimator supposes that observations are independent. If sampling points are too close together, then the distances will be positively correlated.

Consider, for instance, the plot at Ndouantien (we chose the densest plot). The spacing a between sampling plots was varied between 1 and 20 m. For each spacing, the correlation between the distance X_4 measured at a given sampling point and the distance measured at the next sampling point was computed. As expected, the correlation declined as a increased, and stabilized around zero for $a \geq 8$ m. The correlation was significantly positive at the 5% level until $a = 6$ m (same result using both Spearman and Kendall correlation coefficients). We thus elected a minimum spacing of 8 m between sampling points to ensure that distance measurement were independent.

Spacing of 8 m resulted in a sample of 55 distances (we removed all sampling points where distance to the nearest plot border was less than X_4). The mean distance was 3.2 m and its standard deviation 1.3 m. The moment estimator of order -2 yielded the estimate $\hat{\lambda}_{-2} = 1730$ ha^{-1}. The initial values of μ, ω, and R were computed from these values using Equations 9–11, which produced: $\mu_{init} = 7.987$, $\omega_{init} = 216$ ha^{-1}, and $R_{init} = 6.41$ m. These initial values were injected together with the sample of 55 distances into the Nelder–Mead algorithm to maximize the approximate likelihood. Finally, estimates of μ, ω, and R gave $\hat{\mu} = 5.353$, $\hat{\omega} = 298$ ha^{-1}, and $\hat{R} = 1.89$ m (compare with Table 4). The resulting density estimate was $\hat{\omega}\hat{\mu} = 1,594$ ha^{-1}, compared with the real value that was 1,486 ha^{-1} (Table 2).

Effect of Sample Size

As the size n of the distance sample increased, the variance of the estimator $\hat{\omega}\hat{\mu}$ decreased, whereas its bias remained approximately constant. Estimates of the $\hat{\omega}\hat{\mu}$ standard deviation were computed for different values of n by splitting the simulated sample of 10,000 distances into $\lfloor 10{,}000/n \rfloor$ samples of size n, where $\lfloor x \rfloor$ is the greatest integer smaller than x. Figure 2 shows the estimated standard deviation (σ) of $\hat{\omega}\hat{\mu}$ times $\sqrt{n}$ for the ten reference point processes, as a function of n. This shows that $\sqrt{n}\sigma$ was approximately constant.

Estimator Comparisons by Simulation

Table 5 gives the numerical values for the standardized root squared error for each of the eight estimators and for each of the ten benchmark point processes. The proposed estimator $\hat{\omega}\hat{\mu}$ showed the lowest standardized root squared

Table 5. Numerical values for the standardized root squared error $\rho(\hat{\lambda})$ for each of the eight estimators and each of the ten benchmark point processes

	Estimator							
Process	$\hat{\omega}\hat{\mu}$	$\hat{\lambda}_{-2}$	$\hat{\lambda}_2$	$\hat{\lambda}_{KM}$	$\hat{\lambda}_4$	$\hat{\lambda}_5$	$\hat{\lambda}_6$	$\hat{\lambda}_7$
Matérn (5, 100, 5)	0.1615	0.2176	0.3159	0.2349	0.4008	0.1499	0.1468	0.1470
Matérn (2, 100, 5)	0.3264	0.6337	0.3623	0.3111	0.3732	0.4603	0.5669	0.5922
Matérn (1, 500, 1)	0.2044	0.3446	0.1314	0.1232	0.1263	0.3058	0.3127	0.3213
Poisson ($\lambda = 500$)	0.0835	0.0921[a]	0.0725[b]	0.0888[c]	0.0675[b]	0.2414	0.2231	0.2201
Sokouna	0.1292	0.1490	0.3092	0.2631	0.5858	0.1630	0.1551	0.1547
Korokoro	0.1327	0.1843	0.1306	0.1075	0.1348	0.1921	0.1938	0.1983
Ndouantien	0.1311	0.1718	0.2013	0.1451	0.2085	0.1456	0.1540	0.1566
Kokani	0.1337	0.1774	0.1444	0.1125	0.1545	0.2188	0.2243	0.2293
Woro	0.1931	0.3421	0.1782	0.1394	0.1872	0.3084	0.3160	0.3258
Amba	0.1444	0.4045	0.1468	0.1487	0.1434	0.3877	0.3936	0.4063

[a] The theoretical bias is zero and the standardized standard deviation is $1/\sqrt{n(p-2)}$, where $n = 50$ and $p = 4$, giving $\rho = \sigma/\lambda = 0.1$.
[b] The theoretical bias is zero and the standardized standard deviation is $1/\sqrt{np - 2}$, where $n = 50$ and $p = 4$, giving $\rho = \sigma/\lambda = 0.0711$.
[c] The theoretical bias is zero and the standardized standard deviation is $1/\sqrt{np - 2}$, where $n = 50$ and $p = 3$, giving $\rho = \sigma/\lambda = 0.0822$.

error for the Matérn processes at Sokouna and Ndouantien. An estimator with a lower standardized root squared error than $\hat{\omega}\hat{\mu}$ could always be found for the other processes, but this varied from one process to another. Ratios of the estimates provided by each of the other seven estimators and the $\hat{\omega}\hat{\mu}$ estimator were computed for each point process. The mean value of the ratios over the 10-point processes then provided an efficiency index. By construction, this index was one for $\hat{\omega}\hat{\mu}$. The lower the index, the most efficient the estimator. The estimator $\hat{\omega}\hat{\mu}$ came first and was followed by $\hat{\lambda}_{KM}$ (index of 1.06), $\hat{\lambda}_2$ (1.25), $\hat{\lambda}_T$ (1.53), $\hat{\lambda}_{-2}$ (1.58), $\hat{\lambda}_5$ (1.64), $\hat{\lambda}_6$ (1.67), and $\hat{\lambda}_7$ (1.70).

Table 5 is complemented with Figure 3 that plots the standardized standard deviation versus the standardized bias for each process and each estimator. In this plot, the standardized root squared error is given by the distance from the origin. For a given estimator, the points corresponding to the different processes more or less line up. The slope of this line may be interpreted as a trade-off between bias and variance: estimators with a small slope, such as $\hat{\lambda}_{KM}$, $\hat{\lambda}_2$, $\hat{\lambda}_T$, tend to have a high bias but a small variance; estimators with a high slope, such as $\hat{\lambda}_{-2}$ or $\hat{\omega}\hat{\mu}$, tend to have a small bias but a high variance. The proposed estimator $\hat{\omega}\hat{\mu}$ is actually the one with the highest slope.

When considering the detailed characteristics of the point processes, it may be noted that $\hat{\omega}\hat{\mu}$ is comparatively efficient for strongly clustered patterns. Only the Kendall–Moran estimator performed comparably. The estimator $\hat{\omega}\hat{\mu}$ was characterized by a small bias. With the other estimators, this bias could reach high values. For the Matérn process with parameters (2, 100, 5), the standardized bias was about 50% for three estimators. The estimator $\hat{\omega}\hat{\mu}$ was also fairly efficient for the Poisson process. A homogeneous Poisson process with intensity λ can be seen as the limit of a Matérn process with parameters $(R, \omega, \lambda/\omega)$ as $\omega \to 0$ and $\omega R \to \infty$ (and thus $R \to \infty$). Equation 4 then implies $k \to \infty$. From Equation 3, it can be computed that $\lim_{k \to \infty} p_i(x) = m^i e^{-m}/i!$, which is equal to a Poisson distribution with parameter m. The estimator $\hat{\omega}\hat{\mu}$ then converged toward the maximum likelihood estimator of a Poisson process, equal to $\hat{\lambda}_2 \times np/(np - 1)$ (Morisita 1954). We can therefore

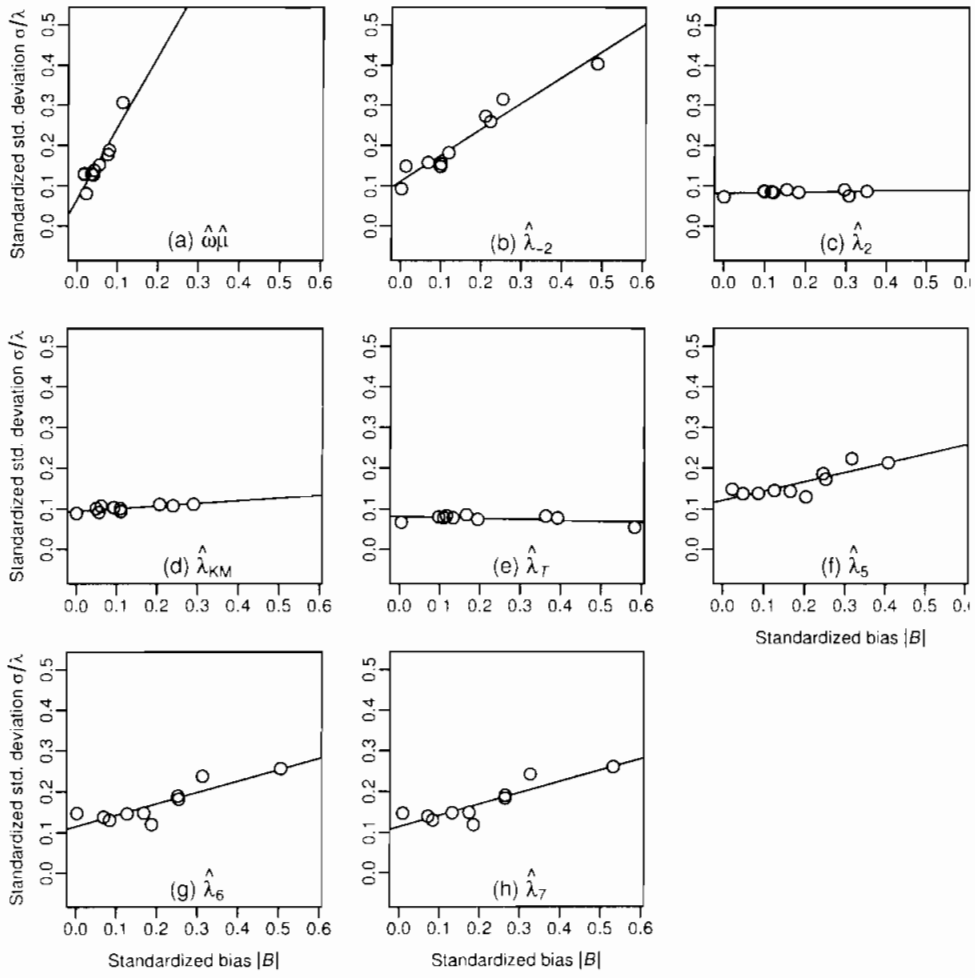

Figure 3. Standardized standard deviation versus the absolute value of the standardized bias: (a) $\hat{\omega}\hat{\mu}$, (b) $\hat{\lambda}_{-2}$, (c) $\hat{\lambda}_2$, (d) $\hat{\lambda}_{KM}$, (e) $\hat{\lambda}_T$, (f) $\hat{\lambda}_5$, (g) $\hat{\lambda}_6$, (h) $\hat{\lambda}_7$. The ten points on each plot correspond to the ten benchmark processes. The distance from the origin gives the standardized root squared error. Lines are regression lines.

expect that, for a homogeneous Poisson process, the standardized bias of $\hat{\omega}\hat{\mu}$ would be close to $1/(np - 1)$ and its standardized standard deviation would be close to $np/[(np - 1)\sqrt{np-2}]$. For $n = 50$ and $p = 4$, this gives $B = 0.005$ and $\sigma/\lambda = 0.071$.

Finally, Figure 4 compares the areas requiring exploration to obtain the measurements for each estimator. Estimators $\hat{\omega}\hat{\mu}$, $\hat{\lambda}_2$, $\hat{\lambda}_{-2}$, and $\hat{\lambda}_T$ required the largest areas, estimators $\hat{\lambda}_5$, $\hat{\lambda}_6$, $\hat{\lambda}_7$ required the smallest, and $\hat{\lambda}_{KM}$ laid in between.

Discussion

Estimators Comparisons

The proposed estimator $\hat{\omega}\hat{\mu}$ had, on average, the lowest standardized root squared error for the benchmark processes. It was followed by the Kendall–Moran estimator. The efficiency shown by $\hat{\lambda}_{KM}$ confirmed the conclusions drawn by Engeman et al. (1994). Conversely, the low efficiency of $\hat{\lambda}_{-2}$ was somewhat surprising because this estimator is recognized for its robustness in the literature (Persson 1964, Eberhardt 1967, Payandeh and Ek 1986, Jonsson et al. 1992, Lessard et al. 2002). The bias of $\hat{\lambda}_{-2}$ noted here does not contradict Eberhardt's (1967) result because his demonstration of the nonbias of $\hat{\lambda}_{-2}$ for a negative binomial distribution with parameters m and k supposed that the shape parameter k was independent of the size of the plot. In the present case, k in fact does depend on plot size (Equation 4). The estimator $\hat{\omega}\hat{\mu}$ showed a low bias (and a comparatively high variance), whereas $\hat{\lambda}_{KM}$ showed a small variance (and a comparatively high bias). Very large samples (here $n = 50$) would therefore be expected to show even better behavior of $\hat{\omega}\hat{\mu}$ as compared with the other estimators.

These results should nevertheless be tempered by several considerations. First, the statistical efficiencies can only be compared realistically if the estimators require the same effort in the field. Field effort may first be assessed by the total area inventoried (or the sampling rate). For a fixed sample size ($n = 50$ in the present case), it is sufficient to compare the mean size of the sampling plots. Figure 4 thus moderates the results of Table 5. A new efficiency estimate may be defined as the product of the standardized error ρ^2 by the mean area to explore at a sampling point (Lynch and Rusydi 1999, Lessard et al. 1994). Again, for each point process, the ratios between the estimates produced by the other seven estimators and $\hat{\omega}\hat{\mu}$ may be computed, and the average of the ratios over the 10 processes provides an efficiency index. In this case the Kendall–Moran estimator came first (efficiency index of 0.90), and was followed by $\hat{\omega}\hat{\mu}$ (1 by construction), $\hat{\lambda}_5$ (1.59), $\hat{\lambda}_6$ (1.65), $\hat{\lambda}_7$ (1.72), $\hat{\lambda}_2$ (1.83), $\hat{\lambda}_{-2}$ (2.74), and $\hat{\lambda}_T$ (5.12).

Field effort may better be assessed as the time required for the inventory, related to the cost of the inventory (Lindsey et al. 1958). The simulations presented here do not address on this question, and the present study should thus be completed by a field study where measurement times are estimated. Nevertheless, it should be noted that $\hat{\lambda}_2$, $\hat{\lambda}_{-2}$, and $\hat{\omega}\hat{\mu}$ required the same time because they required the same measurements. At each sampling point, all three required identification of the fourth nearest tree and measurement of one distance. The estimators $\hat{\lambda}_5$, $\hat{\lambda}_6$, and $\hat{\lambda}_7$ required identification of the two nearest trees and measurement of two distances. Moreover, because it is more difficult to measure T than Z (Figure 1 e and f), $\hat{\lambda}_6$ and $\hat{\lambda}_7$ would take longer than $\hat{\lambda}_5$, whereas $\hat{\lambda}_5$ is already more efficient than $\hat{\lambda}_6$ and $\hat{\lambda}_7$. The Kendall–Moran estimator is not, strictly speaking, a distance-based estimator because it requires the measurement of an area. Thus, it should rather be associated with surface-based estimators (Fraser 1977, Ward 1991, Lowell 1997). At the order $p = 3$, $\hat{\lambda}_{KM}$ requires the identification of the three nearest trees and the measurement of at least three distances and three angles. It may thus be expected to take the longest time. Finally, $\hat{\lambda}_T$ requires the identification of the fourth nearest tree, the measurement of one distance and, probably the longest task, delimitation of each side of the transect.

The second consideration tempering the results is the limited variety of benchmark point processes used to compare the estimators. Although the Matérn process group offers great variability, from random to very clustered patterns, and could be adjusted to all our sites in Mali, further work is required to assess the estimator $\hat{\omega}\hat{\mu}$ with other types of clustering point processes. We may expect other estimators, in particular those developed by Clayton and Cox (1986), to show acceptable behavior in a wider range of point processes than $\hat{\omega}\hat{\mu}$. Thus, $\hat{\omega}\hat{\mu}$ should not be used if the tree spatial pattern is entirely unknown.

Finally, our results did not consider measurement errors. The simulations did not take account of measurement errors, and again a field study would be required for their assessment. Measurement errors that inflate estimator variance are likely to increase with the complexity of the measurements.

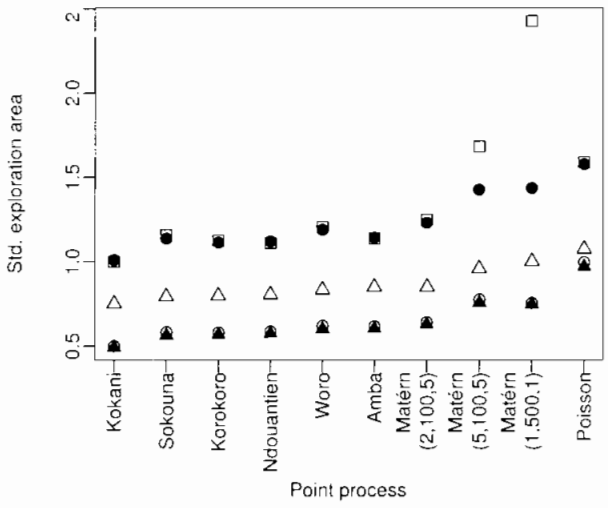

Figure 4. Mean exploration area to obtain the measurements at a sampling point, divided by p/λ ($p = 4$), where λ is the point process intensity. p/λ is the area of the plot on which, on average, p trees would be found, so that the ratio is a "standardized" exploration area. The x-axis is nominal and simply gives point process names. Black dots refer to $\hat{\omega}\hat{\mu}$, $\hat{\lambda}_2$, and $\hat{\lambda}_{-2}$; white squares refer to $\hat{\lambda}_T$; white triangles refer to $\hat{\lambda}_{KM}$; black triangles refer to $\hat{\lambda}_5$; and finally white dots refer to $\hat{\lambda}_6$ and $\hat{\lambda}_7$.

$\hat{\lambda}_{KM}$ and $\hat{\lambda}_I$ would therefore be expected to yield the largest measurement errors.

Estimating Other Characteristics

This study focused on the estimation of tree density. Estimating additional characteristics, such as basal area or volume or qualitative quantities such as the density of each species, would require specific approaches. The quantitative or qualitative characteristics of a forest stand may be modeled using a marked point process (Cressie 1991, Penttinen et al. 1992), the mark being either quantitative or qualitative. In all cases, the "density" m of the mark may be estimated in a distance-based approach by a ratio of the means $(\Sigma_{i=1}^{n} M_i)/(\Sigma_{i=1}^{n} S(D_i))$ or by a mean of the ratios $(1/n)\Sigma_{i=1}^{n}(M_i/S(D_i))$, where $S(D)$ is the area of the sampling plot computed from the distance D, and M_i is the sum of the marks over the p trees in plot i: $M_i = \Sigma_{j=1}^{p} m_{ij}$, where m_{ij} is the mark of the jth tree in the ith sampling plot.

To estimate tree density, one simply has to set $m_{ij} = 1$ for all i and j; to estimate the density of a given species, one has to set $m_{ij} = 1$ if the corresponding tree belongs to the desired species, and 0 otherwise; to estimate basal area, one has to set m_{ij} equal to the basal area of the corresponding tree; etc. Estimators of the "ratio of the means" type were used by Jonsson et al. (1992) and Schreckenberg (1996) to estimate quantitative characteristics, whereas estimators of the "mean of the ratios" type were used by Mawson (1968), Prodan (1968), Jonsson et al. (1992), Lessard et al. (1994), Lynch and Rusydi (1999). For qualitative characteristics, say a species, $\hat{f}_i = M_i/p$ is an estimator of species frequency in plot i, and $\hat{f} = (\Sigma_{i=1}^{n} M_i)/(np)$ is an estimator of species frequency in the entire stand. The ratio of the means estimator can then be written as $\hat{f}\hat{\lambda}$, and the mean of the ratios estimator can be written as $(1/n)\Sigma_{i=1}^{n} \hat{f}_i\hat{\lambda}_i$, where $\hat{\lambda} = p/[\Sigma_{i=1}^{n} S(D_i)/n]$ and $\hat{\lambda}_i = p/S(D_i)$ are estimators of total density (all species), either at the stand level or at the plot level. The approach thus consists of estimating total density then splitting it up between species (Schreckenberg 1996). An alternative would be to apply a density estimator, ignoring the trees of the unwanted species. This can actually result in large distances to measure, unless truncated distance-based estimators are used (Batcheler 1971, Keuls et al. 1963, Sheil et al. 2003).

The difficulty in estimating the density of a mark using distance-based methods is that the dependence between the marks and the location of the trees affects the output. For instance, consider the following pattern

repeated on a square grid, where black and white dots stand for two species. Provided that the side of the grid is far larger than the distances between trees within the pattern, an estimate of the species frequencies based on a sampling plot with radius X_4 (Figure 1a) would yield $\hat{f}_{\bullet} \simeq 1/4$ and $\hat{f}_{\circ} \simeq 3/4$, whereas the true values are $f_{\bullet} = 1/5$ and $f_{\circ} = 4/5$. Hence, designing an unbiased distance-based estimator would require characterizing the departure from random labeling (Goreaud and Pélissier 2003). Moreover, if the estimator is to be evaluated using simulated spatial patterns, a realistic simulation of the marked point processes is required. This is left for future work.

Conclusion

When considering Matérn point processes, the proposed tree density estimator $\hat{\omega}\hat{\mu}$ of the tree density is efficient in terms of bias and variance. The Kendall–Moran estimator is also efficient. This conclusion does not take account of field effort or measurement errors. When the sampling rate is taken into account, the Kendall–Moran estimator is more efficient than $\hat{\omega}\hat{\mu}$. However, $\hat{\lambda}_{KM}$ requires more complex measurements that take longer and the measurement errors are larger. The extension of $\hat{\omega}\hat{\mu}$ to estimate additional or qualitative stand characteristics warrants further work.

Literature Cited

ABRAMOWITZ, M., AND I.A. STEGUN. 1964. Handbook of mathematical functions (with formulas, graphs, and mathematical tables). US Government Printing Office, Washington, DC.

AHERNE, W.A., AND P.J. DIGGLE. 1978. The estimation of neuronal population density by a robust distance method. J. Microscop. 114:285–293.

BATCHELER, C.L. 1971. Estimation of density from a sample of joint point and nearest-neighbor distances. Ecology 52:703–709.

BYTH, K. 1982. On robust distance-based intensity estimators. Biometrics 38:127–135.

CATANA, A.J.J. 1963. The wandering quarter method of estimating population density. Ecology 44:349–360.

CLAYTON, G., AND T.F. COX. 1986. Some robust density estimators for spatial point processes. Biometrics 42:753–767.

CONSEIL SCIENTIFIQUE POUR L'AFRIQUE (CSA). 1956. Réunion Yangambi sur la classification des formations végétales de l'Afrique. Commission de Coopération Technique en Afrique au sud du Sahara, Londres, UK. Publication 22. 35 p.

COTTAM, G., AND J.T. CURTIS. 1956. The use of distance measures in phytosociological sampling. Ecology 37:451–460.

COX, T.F. 1976. The robust estimation of the density of a forest stand using a new conditioned distance method. Biometrika 63:493–499.

CRESSIE, N. 1991. Statistics for spatial data. John Wiley & Sons, New York. 900 p.

DIGGLE, P.J. 1975. Robust density estimation using distance methods. Biometrika 62:39–48.

DIGGLE, P.J. 1977. A note on robust density estimation for spatial point patterns. Biometrika 64:91–95.

EBERHARDT, L.L. 1967. Some developments in distance sampling. Biometrics 23:207–216.

ENGEMAN, R.M., AND R.T. SUGIHARA. 1998. Optimization of variable area transect sampling using Monte Carlo simulation. Ecology 79:1425–1434.

ENGEMAN, R.M., R.T. SUGIHARA, L.F. PANK, AND W.E. DUSENBERRY. 1994. A comparison of plotless density estimators using Monte Carlo simulation. Ecology 75:1769–1779.

FRASER, A. 1977. Triangle-based probability polygons for forest sampling. For. Sci. 23:111–121.

GORIAUD, F., AND R. PELISSIER. 2003. Avoiding misinterpretation of biotic interactions with the intertype K12-function: Population independence vs. random labelling hypotheses. J. Veg. Sci. 14:681–692.

HOLGATE, P. 1964. The efficiency of nearest neighbour estimators. Biometrics 20:647–649.

HOLGATE, P. 1965A. The distance from a random point to the nearest point of a closely packed lattice. Biometrika 52:261–263.

HOLGATE, P. 1965B. Tests of randomness based on distance methods. Biometrika 52:345–353.

JONSSON, B., S. HOLM, AND H. KALLUR. 1992. A forest inventory method based on density-adapted circular plot size. Scand. J. For. Res. 7:405–421.

KENDALL, M.G., AND P.A.P. MORAN. 1963. Geometrical probability. Griffin, London, UK. 125 p.

KEUTS, M., H.J. OVER, AND C.T. DE WIT. 1963. The distance method for estimating densities. Statist. Neerl. 17:71–91.

KOUYATE, A.M. 1995. Contribution à l'étude de méthode d'estimation rapide du volume dans les formations savanicoles: Cas du terroir villageois de Siani au Mali. M.Sc. thesis, Univ. of Antananarivo, Antananarivo, Madagascar. 48 p.

LESSARD, V., D.D. REED, AND N. MONKEVICH. 1994. Comparing *n*-tree distance sampling with point and plot sampling in northern Michigan forest types. North. J. Appl. For. 11:12–16.

LESSARD, V.C., T.D. DRUMMER, AND D.D. REED. 2002. Precision of density estimates from fixed-radius plots compared to *n*-tree distance sampling. For. Sci. 48:1–6.

LEWIS, S.M. 1975. Robust estimation of density for a two-dimensional point process. Biometrika 62:519–521.

LINDSEY, A.A., J.D.J. BARTON, AND S.R. MILES. 1958. Field efficiencies of forest sampling methods. Ecology 39:428–444.

LOWELL, K.E. 1997. An empirical evaluation of spatially based forest inventory samples. Can. J. For. Res. 27:352–360.

LYNCH, T.B., AND R. RUSYDI. 1999. Distance sampling for forest inventory in Indonesian teak plantations. For. Ecol. Manag. 113:215–221.

MAWSON, J.C. 1968. A Monte Carlo study of distance measures in sampling for spatial distribution in forest stands. For. Sci. 14:127–139.

MOORE, P.G. 1954. Spacing in plant populations. Ecology 35:222–227.

MORISITA, M. 1954. Estimation of population density by spacing method. Mem. Fac. Sci. Kyushu Univ. Ser. E, 1:187–197.

MORISITA, M. 1957. A new method for the estimation of density by the spacing method applicable to non-randomly distributed populations. Physiol. Ecol. 7:134–144.

NASI, R., AND M. SABATIER. 1988. Projet Inventaire des Ressources Ligneuses au Mali: les formations végétales. Ministère chargé des ressources naturelles et de l'élevage, Direction nationale des eaux et forêts/BDPA/SCET-AGRI/CTFT, Bamako, Mali, Rapport de synthèse, première phase. 205 p.

NELDER, J.A., AND R. MEAD. 1965. A simplex algorithm for function minimization. Comput. J. 7:308–313.

NOUVELLET, Y., M.L. SYLLA, AND A. KASSAMBARA. 2000. Détermination de la productivité des jachères dans la zone de Cinzana (Mali). P. 475–483 *in* La jachère en Afrique tropicale: Rôles, aménagement, alternatives, Floret, C. and R. Pontanier (eds.), Vol. 1. Éditions John Libbey Eurotext, Paris, France.

PARKER, K.R. 1979. Density estimation by variable area transect. J. Wildl. Manag. 43:484–492.

PATIL, S.A., K.P. BURNHAM, AND J.L. KOVNER. 1979. Non-parametric estimation of plant density by the distance method. Biometrics 35:597–604.

PATIL, S.A., J.L. KOVNER, AND K.P. BURNHAM. 1982. Optimum non-parametric estimation of population density based on ordered distances. Biometrics 38:243–248.

PAYANDEH, B., AND A.R. EK. 1986. Distance methods and density estimators. Can. J. For. Res. 16:918–924.

PENTTINEN, A., D. STOYAN, AND H.M. HENTTONEN. 1992. Marked point processes in forest statistics. For. Sci. 38:806–824.

PERSSON, O. 1964. Distance methods. The use of distance measurements in the estimation of seedling density and open space frequency. Stud. For. Suec. 15:1–68.

PERSSON, O. 1971. The robustness of estimating density by distance measurements. P. 175–190 *in* Statistical ecology: Sampling and modeling biological populations and population dynamics, Patil, G.P., E.C. Pielou, and W.E. Waters (eds.), Vol. 2. Pennsylvania Univ. Press, Univ. Park, PA.

POLLARD, J.H. 1971. On distance estimators of density in randomly distributed forests. Biometrics 27:991–1002.

PRODAN, M. 1968. Punktstichprobe für die forsteinrichtung. Forst. und Holzwirt 23:225–226.

R DEVELOPMENT CORE TEAM. 2003. R: A language and environment for statistical computing. R Foundation for Statistical Computing, Vienna, Austria. 1029 p.

SCHRECKENBERG, K. 1996. Forests, fields and markets: A study of indigenous tree products in the woody savannas of the Bassila region, Benin. Ph.D. thesis, Univ. of London, London, UK. 326 p.

SHEIL, D., M.J. DUCEY, K. SIDIYASA, AND I. SAMSOEDIN. 2003. A new type of sample unit for the efficient assessment of diverse tree communities in complex forest landscapes. J. Trop. For. Sci. 15:117–135.

SMALTSCHINSKI, T.K. 1981. Density and spatial patterns of forest stand. Ph.D. thesis, Albert Ludwig Univ., Freiburg in Brisgau, Germany. 127 p.

STOYAN, D., AND H. STOYAN. 1994. Fractals, random shapes and point fields. John Wiley & Sons, Chichester, U.K. 390 p.

SYLLA, M.L. 1997. Évaluation rapide de la productivité et de la production des formations végétales: Bassins de Bamako et de

Ségou. République du Mali, Ministère des mines, de l'énergie et de l'hydraulique, and Ministère du développement rural et de l'environnement, Bamako, Mali. Rapport de mission. 27 p.

THOMPSON, H.R. 1956. Distribution of distance to *n*th neighbour in a population of randomly distributed individuals. Ecology 37:391–394.

WARD, D. 1991. Triangular tessellation: A new approach to forest inventory. For. Ecol. Manage. 44:285–290.